ORGANIC LETTERS

2006
Vol. 8, No. 19
4255−4258

Carotenoid Radical Anions and Their Protonated Derivatives

Ali El-Agamey,*,†,‡ Ruth Edge,*,‡,§ Suppiah Navaratnam,§,|| Edward J. Land,‡ and T. George Truscott*,‡

School of Physical and Geographical Sciences, Keele University, Keele, Staffordshire ST5 5BG, UK, Free Radical Research Facility, CCLRC Daresbury Laboratory, Warrington WA4 4AD, UK, and Biosciences Research Institute, University of Salford, Salford M5 4WT, UK

a.a.g.el-agamey@chem.keele.ac.uk; r.edge@dl.ac.uk; t.g.truscott@chem.keele.ac.uk

Received June 16, 2006

ABSTRACT

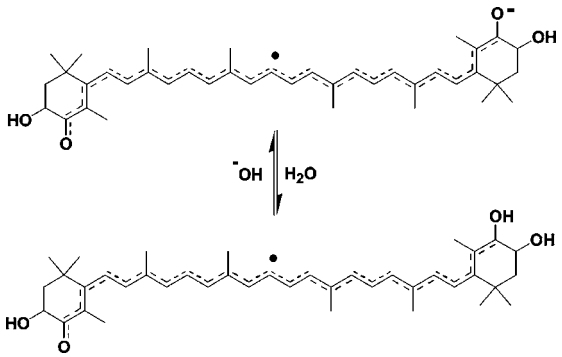

In this study, we report the protonation reactions for astaxanthin and canthaxanthin radical anions in methanol, alkaline methanol, and aqueous 2% Triton X-100 at different pH values. The pK_a values for the corresponding α-hydroxy radical derivatives of astaxanthin, canthaxanthin, and *β*-apo-8′-carotenal were estimated in 2% Triton X-100. Also, the effects of the microenvironment and the structure of the carotenoids on the protonation rate constant are discussed.

An earlier report by Land et al. showed that the radical anions of carbonyl-containing carotenoids can be protonated in methanol to form the corresponding α-hydroxy radical derivatives (equation 1)[1]. In alkaline methanolic solutions, the reaction shifts toward the unprotonated species and only carotenoid radical anions were observed (eq 1)[1].

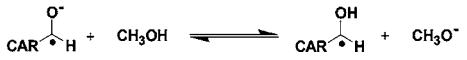

(1)

Similar studies have been reported in other solvents and in micelles.[2−5] In the previous reports there was no detailed study of the influence of pH.[1,4] Also, most of the reported rate constants for the protonation reaction concern only organic solvents.[1−4]

In this study, we report the protonation reactions for the radical anions of the two carotenoids, astaxanthin (ASTA) and canthaxanthin (CAN), for the first time, in methanol, alkaline methanol (containing 0.01 M NaOH) and in aqueous 2% Triton X-100 (TX-100) at pH values over the range 7−13.5. The radical anions of these two dietary carotenoids have not been studied previously in protic solvents. From these data, we obtained the pK_a values for the corresponding α-hydroxy radical derivatives of ASTA, CAN, and *β*-apo-8′-carotenal (APO) in aqueous 2% TX-100. Also, the rate constants for protonation of the radical anions were measured in aqueous 2% TX-100 and in methanol.

† Permanent address: Chemistry Department, Faculty of Science, New Damietta, Damietta, Egypt.
‡ Keele University.
§ CCLRC Daresbury Laboratory.
|| University of Salford.

(1) Land, E. J.; Lafferty, J.; Sinclair, R. S.; Truscott, T. G., *J. Chem. Soc., Faraday Trans. 1* **1978**, *74*, 538.
(2) Raghavan, N. V.; Das, P. K.; Bobrowski, K. *J. Am. Chem. Soc.* **1981**, *103*, 4569.
(3) Bobrowski, K.; Das, P. K. *J. Phys. Chem.* **1985**, *89*, 5733.
(4) Bobrowski, K.; Das, P. K. *J. Phys. Chem.* **1987**, *91*, 1210.

10.1021/ol061484s CCC: $33.50
Published on Web 08/25/2006

Pulse radiolysis is one of the most appropriate techniques to investigate the spectroscopic properties of carotenoid radicals.[1−4,6−8] In argon-saturated water,[8−10] both oxidizing ($^{\bullet}OH$) and reducing (e_{aq}^- and $H^{\bullet}$) species are formed (Scheme 1). To study exclusively reducing conditions we added 0.1

Scheme 1

$$H_2O \rightsquigarrow e_{aq}^- + {}^{\bullet}OH + H^{\bullet} + \text{non-radical species}$$
$$^{\bullet}OH + HCO_2^- \rightarrow H_2O + CO_2^{\bullet-}$$
$$e_{aq}^- + CAR \rightarrow CAR^{\bullet-}$$
$$CO_2^{\bullet-} + CAR \rightarrow CAR^{\bullet-} + CO_2$$
$$e_{aq}^- + H_2O + N_2O \rightarrow N_2 + OH^- + {}^{\bullet}OH$$

M formate; this converts the oxidizing $^{\bullet}OH$ radicals into $CO_2^{\bullet-}$, which is a reducing radical. In the presence of a carotenoid (CAR), $CAR^{\bullet-}$ is formed from both electron attachment (fast reaction) and electron transfer from $CO_2^{\bullet-}$ (slow reaction).[11] In N_2O-saturated solution, e_{aq}^- is converted into $^{\bullet}OH$; therefore, $CAR^{\bullet-}$ is generated only from $CO_2^{\bullet-}$ (Scheme 1). The structures of the carotenoids used are shown in Figure 1.

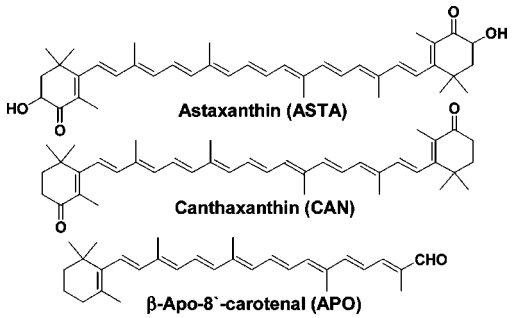

Figure 1. Carotenoid structures.

The transient spectra obtained from pulse radiolysis of ASTA (50 μM) and formate (0.1 M) in aqueous 2% (w/v) TX-100 (argon-saturated, pH = 7.1), in the microsecond time scale, are shown in Figure 2. The short-lived transient (λ_{max} ~730−750 nm) is attributed to $ASTA^{\bullet-}$, generated from fast electron attachment to ASTA, which abstracts a proton from

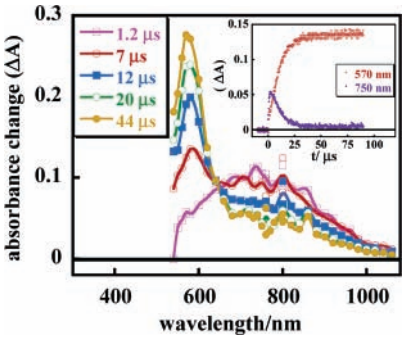

Figure 2. Transient absorption spectra following pulse radiolysis of ASTA (50 μM) and formate in argon-saturated aqueous 2% TX-100 (pH = 7.1). Inset: kinetics of $ASTAH^{\bullet}$ at 570 nm and $ASTA^{\bullet-}$ at 750 nm.

H_2O to form the corresponding α-hydroxy radical derivative ($ASTAH^{\bullet}$) at λ_{max} = 570 nm. Thus, the transient decay at 750 nm matches the transient growth at 570 nm (see Figure 2 inset).

At low ASTA concentration (10 μM), the electron decay, mainly due to the reaction with ASTA, is followed by a subsequent buildup of $ASTAH^{\bullet}$ observed at 570 nm (Figure S1, Supporting Information). It is important to note that the rate of formation of the transient at 570 nm is not dependent on the ASTA concentration, which confirms that this transient is not due to any direct radical reaction with ASTA but is due to the protonation of $ASTA^{\bullet-}$ ($\epsilon = 5.3 \times 10^4$ M^{-1} cm^{-1} at 720 nm, see the Supporting Information). The rate constant for the protonation of $ASTA^{\bullet-}$ by water was estimated as 1.9×10^3 M^{-1} s^{-1} [12] from the growth of $ASTAH^{\bullet}$ at 570 nm. The $ASTAH^{\bullet}$ ($\epsilon = 8.2 \times 10^4$ M^{-1} cm^{-1} at 570 nm, see the Supporting Information) decays by second-order kinetics ($2k/\epsilon$ = 140 cm s^{-1}), probably via a radical−radical reaction (Figure S2, Supporting Information).

The transient profile at 570 nm shows a slow secondary growth over the millisecond time scale (Figure S3, Supporting Information). This growth can be attributed to the slow electron transfer from $CO_2^{\bullet-}$ to ASTA to form $ASTA^{\bullet-}$, which protonates to form additional $ASTAH^{\bullet}$. In this reaction, the slow growth of $ASTAH^{\bullet}$ is controlled by the slow reaction of $CO_2^{\bullet-}$ with ASTA. This was confirmed by saturating the same solution with N_2O (Figures S4 and S5, Supporting Information).

At pH = 13, the transient spectra of an argon-saturated solution have a band due to $ASTA^{\bullet-}$ (λ_{max} ~730−750 nm, see Figure 3), while $ASTAH^{\bullet}$ formation was not observed. Since there is no protonation at pH = 13, we can obtain the rate constant for the electron attachment ($k_{ASTA + e_{aq}^-} = 3.9 \times 10^9$ M^{-1} s^{-1}) with no correction for the protonation reaction. Furthermore, at this high pH, $ASTA^{\bullet-}$ decays very slowly, by second-order kinetics ($2k/\epsilon$ = 470 cm s^{-1}), probably via a radical−radical reaction (Figure S6, Supporting Information).[2] Also, the buildup of $ASTA^{\bullet-}$ at millisecond time scales was observed due to the reaction of ASTA with $CO_2^{\bullet-}$ (Figure S7, Supporting Information). A similar transient spectrum of $ASTA^{\bullet-}$ was observed

(5) Konovalova, T. A.; Kispert, L. D.; Polyakov, N. E.; Leshina, T. V. *Free Rad. Biol. Med.* **2000**, *28*, 1030.
(6) (a) Lafferty, J.; Roach, A. C.; Sinclair, R. S.; Truscott, T. G.; Land, E. J. *J. Chem. Soc., Faraday Trans. 1* **1977**, *73*, 416. (b) Conn, P. F.; Lambert, C.; Land, E. J.; Schalch, W.; Truscott, T. G. *Free Rad. Res. Commun.* **1992**, *16*, 401. (c) Bobrowski, K.; Das, P. K. *J. Phys. Chem.* **1985**, *89*, 5079. (d) Lo, K. K. N.; Land, E. J.; Truscott, T. G. *Photochem. Photobiol.* **1982**, *36*, 139. (e) Lafferty, J.; Truscott, T. G.; Land, E. J. *J. Chem. Soc., Faraday Trans. 1* **1978**, *74*, 2760.
(7) Dawe, E. A.; Land, E. J. *J. Chem. Soc., Faraday Trans. 1* **1975**, *71*, 2162.
(8) Hill, T. J.; Land, E. J.; McGarvey, D. J.; Schalch, W.; Tinkler, J. H.; Truscott, T. G. *J. Am. Chem. Soc.* **1995**, *117*, 8322.
(9) Hill, T. J. Molecular Mechanisms of Photoprotection. Ph.D. Thesis, Keele University, 1994, pp 212−222.
(10) Bensasson, R. V.; Land, E. J.; Truscott, T. G. *Flash photolysis and pulse radiolysis: Contributions to the chemistry of biology and medicine;* Pergamon Press: Oxford, 1983; pp 1−19 and 67−92.
(11) Wardman, P. *J. Phys. Chem. Ref. Data* **1989**, *18*, 1637.

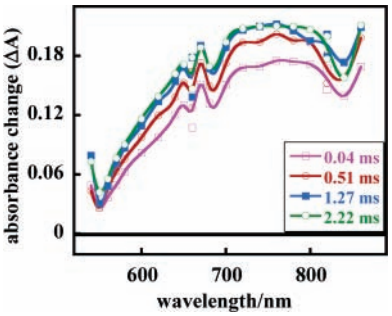

Figure 3. Transient absorption spectra following pulse radiolysis of ASTA (50 μM) and formate in argon-saturated aqueous 2% TX-100 (pH = 13).

from the reaction of acetone ketyl radical ($AC^{\bullet-}$) with ASTA ($k_{ASTA + AC^{\bullet-}} = 2.3 \times 10^8\ M^{-1}\ s^{-1}$) in N_2O-saturated aqueous 2% TX-100 containing 0.1 M 2-propanol at pH = 13 (Scheme S1 and Figures S8 and S9, Supporting Information). This reaction is efficient because of the low reduction potential of acetone.[11]

In argon-saturated solutions, containing formate, the influence of pH on the yield of $ASTAH^{\bullet}$ (at 570 nm) at microsecond time scales[13] is shown in Figure 4. From the

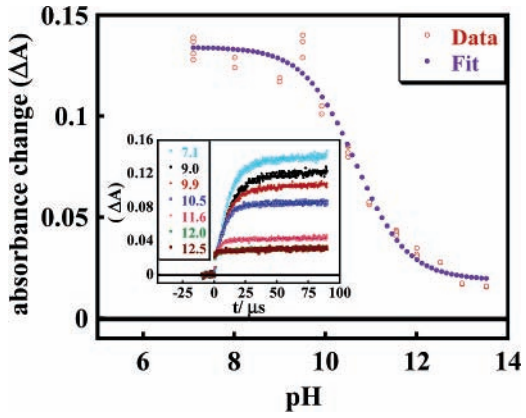

Figure 4. ΔA versus pH for $ASTAH^{\bullet}$ (at 570 nm) following pulse radiolysis of ASTA (50 μM) and formate in argon-saturated aqueous 2% TX-100. Inset: kinetics of $ASTAH^{\bullet}$ (at 570 nm) at different pH values.

plot of pH versus the yield of $ASTAH^{\bullet}$ at microsecond or millisecond time scales (Figure S10, Supporting Information),[13] the pK_a of $ASTAH^{\bullet}$ was estimated as 10.6 ± 0.2.

In addition, the protonation reaction of $ASTA^{\bullet-}$ has been studied in argon-saturated methanol (Figure S11, Supporting Information). Under these conditions, $ASTA^{\bullet-}$ is generated from the reaction of ASTA with the electron. Once formed, $ASTA^{\bullet-}$ rapidly abstracts a proton from methanol ($k = 4.9 \times 10^4\ M^{-1}\ s^{-1}$) to form $ASTAH^{\bullet}$ (λ_{max} = 550 nm). In N_2O-saturated solution, no formation of $ASTA^{\bullet-}$ was observed, which indicates that $ASTA^{\bullet-}$ is more reducing than hydroxymethyl radical ($HOCH_2^{\bullet}$). In methanol containing 0.01 M NaOH (Figures S12 and S13, Supporting Information), only $ASTA^{\bullet-}$ is produced (λ_{max} ~610−620 nm) via a fast (electron attachment) and a slow (reaction of $^{\bullet}CH_2O^-$ with ASTA) formation, as shown in Scheme 2 and Figure S14 (Supporting Information).

Scheme 2

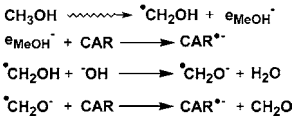

Similar trends were observed with canthaxanthin in argon-saturated aqueous 2% TX-100 containing formate at pH = 7.1 (Figure S15, Supporting Information). $CAN^{\bullet-}$ (λ_{max} ~730−740 nm, $\epsilon = 2.1 \times 10^4\ M^{-1}\ cm^{-1}$ at 720 nm (see the Supporting Information)) decays to the α-hydroxy radical derivative ($CANH^{\bullet}$) (λ_{max} = 580 nm) via a protonation reaction ($k_{CAN^{\bullet-} + H_2O} = 4.0 \times 10^3\ M^{-1}\ s^{-1}$). The $CANH^{\bullet}$ ($\epsilon = 3.4 \times 10^4\ M^{-1}\ cm^{-1}$ at 570 nm, see the Supporting Information) decays very slowly via second-order kinetics (Figure S16 (Supporting Information), $2k/\epsilon = 200\ cm\ s^{-1}$). Also, a secondary growth was observed at 570 nm, at millisecond time scales, due to the reaction of $CO_2^{\bullet-}$ with CAN (Figure S17, Supporting Information). This was confirmed by investigating the same reaction mixture in N_2O-saturated solution (Figure S18, Supporting Information).

At pH = 13, in argon-saturated solution, only the transient spectra of $CAN^{\bullet-}$ (Figure S19, Supporting Information) were observed. Similar transient spectra for $CAN^{\bullet-}$ (Figures S20−S22, Supporting Information) were obtained via the reaction of $AC^{\bullet-}$ with CAN in N_2O-saturated solution ($k_{CAN + AC^{\bullet-}} = 2.7 \times 10^8\ M^{-1}\ s^{-1}$). From the plot of pH versus the yield of $CANH^{\bullet}$ at microsecond or millisecond time scales (Figures 5 and S23, Supporting Information),[13] the pK_a of $CANH^{\bullet}$ was estimated as 11.7 ± 0.2.

In argon-saturated methanol, the initially formed $CAN^{\bullet-}$ converts into $CANH^{\bullet}$ (λ_{max} = 550 nm) via proton abstraction ($k = 5.3 \times 10^4\ M^{-1}\ s^{-1}$) from methanol (Scheme 2 and Figure S24, Supporting Information). In N_2O-saturated solution, no formation of $CAN^{\bullet-}$ was observed. In methanol containing 0.01 M NaOH, as for ASTA, fast and slow formation of $CAN^{\bullet-}$ (λ_{max} ~600−610 nm) is observed due to electron and $^{\bullet}CH_2O^-$ reactions (Figures S25−S27, Supporting Information, and Scheme 2).

Pulse radiolysis of β-apo-8′-carotenal in argon-saturated aqueous 2% TX-100 containing formate at pH = 7.2 (Figures 6 and S28, Supporting Information), generates $APO^{\bullet-}$ (λ_{max} ~590−600 nm), which protonates rapidly ($k = 760\ M^{-1}\ s^{-1}$) to $APOH^{\bullet}$ (λ_{max} = 510 nm).

(12) The standard errors for all the reported rate constants and molar absorption coefficients are ±15% unless otherwise stated.

(13) At microsecond time scales, the yield represents $CARH^{\bullet}$ generated from the protonation of $CAR^{\bullet-}$, which was formed from the electron attachment only. At millisecond time scales, the yield represents $CARH^{\bullet}$ generated from the protonation of $CAR^{\bullet-}$, which was formed the reactions of CAR with both electron and $CO_2^{\bullet-}$.

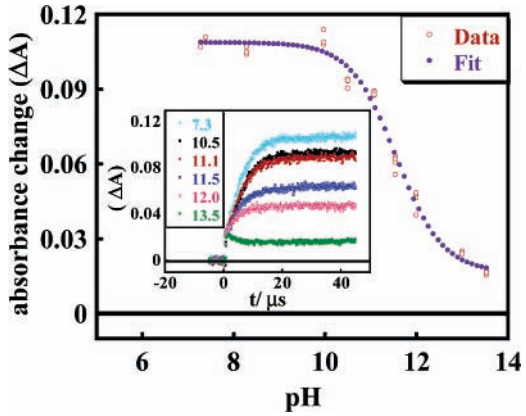

Figure 5. pH versus ΔA of CANH$^{\bullet}$ (at 570 nm) following pulse radiolysis of CAN (32 μM) and formate in argon-saturated aqueous 2% TX-100. Inset: kinetics of CANH$^{\bullet}$ (at 570 nm) at different pH values.

At pH = 13, only APO$^{\bullet-}$ is generated (Figure S29, Supporting Information). Similar spectra have been reported by Bobrowski and Das at high and low pH,[4] but these workers did not study the range of pH values necessary to determine the pK_a. By varying the pH values from 7 to 13.5, we obtained the pK_a of APOH$^{\bullet}$ as 10.2 $\pm$ 0.1. The plots of pH versus the yield of APO$^{\bullet-}$ at microsecond or millisecond time scales are given in Figures S30 and S31 (Supporting Information).

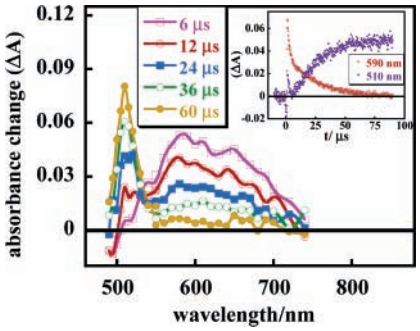

Figure 6. Transient absorption spectra following pulse radiolysis of APO (30 μM) and formate in argon-saturated aqueous 2% TX-100 (pH = 7.2). Inset: kinetics of APOH$^{\bullet}$ at 510 nm and APO$^{\bullet-}$ at 590 nm.

The rate constants for ASTA$^{\bullet-}$ and CAN$^{\bullet-}$ protonation are faster than that of APO$^{\bullet-}$ (Table 1). However, it was reported previously that for model carotenoids containing only one carbonyl group the rate constant for protonation decreases as the chain length increases.[4] This different behavior for the dietary carotenoids could be due to the presence of a carbonyl group in ASTA and CAN at each end of the molecule increasing the probability of the protonation. In addition, the higher rate constants for the protonation of CAR$^{\bullet-}$ in methanol, compared to that in aqueous TX-100, indicate that the TX-100 micelle hinders its reaction with water. Moreover, the rate constant for the protonation of ASTA$^{\bullet-}$ in TX-100 is smaller (by a factor of $\sim$2) than that of CAN$^{\bullet-}$. This rather surprising result could be due to the different orientation of ASTA$^{\bullet-}$ in the TX-100 micelle, induced by the presence of hydroxyl groups, which reduces the carbonyl groups interaction with water.

Table 1. λ_{Max} of CAR$^{\bullet-}$ (and CARH$^{\bullet}$) and Their Protonation Rate Constants in TX-100 and Methanol

	TX-100/nm		methanol/nm	
CAR	CAR$^{\bullet-}$ [a] (k/M^{-1} s^{-1})	CARH$^{\bullet}$	CAR$^{\bullet-}$ [b] (k/M^{-1} s^{-1})	CARH$^{\bullet}$
ASTA	730−750 (1.9×10^3)	570	610−620 (4.9×10^4)	550
CAN	730−740 (4.0×10^3)	580	600−610 (5.3×10^4)	550
APO	590−600 (760)	510	555 (1.6×10^4)[4]	-

[a] Protonation of CAR$^{\bullet-}$ with water ($k_{CAR^{\bullet-} + H_2O}$). [b] Protonation of CAR$^{\bullet-}$ with methanol ($k_{CAR^{\bullet-} + MeOH}$).

The lower pK_a value of ASTAH$^{\bullet}$ (10.62) in TX-100, compared with that of CANH$^{\bullet}$ (11.72), could be due to the inductive effect of the hydroxyl groups in the terminal cyclic rings.

A large blue shift for the λ_{max} of ASTA$^{\bullet-}$ and CAN$^{\bullet-}$ was observed on moving from nonpolar solvents to polar ones. For example, λ_{max} of ASTA$^{\bullet-}$ in hexane, benzene and aqueous 2% TX-100 are 1120,[14] $\geq$1100,[15] and 730−750 nm respectively and λ_{max} of CAN$^{\bullet-}$ in hexane, benzene, and aqueous 2% TX-100 are 1150,[6a] $\geq$1100,[15] and 730−740 nm, respectively. A large blue shift has been reported[1,3,6a,7] for other carotenoids and was attributed to the less uniformly distributed charge in the ground state of CAR$^{\bullet-}$ than that of its first excited state. Therefore, in polar solvents, the ground state is stabilized relative to the excited state. Consequently, the λ_{max} of CAR$^{\bullet-}$ in polar solvents is at shorter wavelengths than in nonpolar solvents.[6a]

Rather similar values of the λ_{max} of CAR$^{\bullet-}$ in methanol and in aqueous TX-100 were observed (Table 1), which indicates that CAR$^{\bullet-}$ is located in a polar environment in the TX-100 micelle.[3,4]

In summary, the protonation of CAR$^{\bullet-}$, which contain one (APO) or two (ASTA and CAN) carbonyl group(s), in aqueous 2% TX-100 and methanol have been observed, and the pK_a values for CARH$^{\bullet}$ have been estimated by monitoring the change of the transient yield with pH.

Acknowledgment. We are grateful to the Leverhulme Trust (Research Grant No. F/00130F) for financial support, to Hoffman La Roche (Vitamins) and Dr Regina Goralczyk (DSM Nuritional Products) for supplying the carotenoids used in this work, and to the Free Radical Research Facility (station 0.1) in the Synchrotron Radiation Department of the CCLRC Daresbury Laboratory, Warrington, UK, for access to the pulse radiolysis facility.

Supporting Information Available: Experimental details and kinetic and spectral data. This material is available free of charge via the Internet at http://pubs.acs.org.

OL061484S

(14) Tinkler, J. H. The Excited States and Radical Ions of the Carotenoids. Ph.D. Thesis, Keele University, 1995, pp 211−230.

(15) Edge, R. Spectroscopic and Kinetic Investigations of Carotenoid Radical Ions and Excited States. Ph.D. Thesis, Keele University, 1998, pp 174−188.